

PLASTIC BUCKLING OF CONICAL TANKS WITH LARGE GEOMETRICAL IMPERFECTIONS

Guy A. M. E. Lagae*, Wesley M. H. Vanlaere* and Rudy E. Van Impe*

* Department of Structural Engineering, Ghent University
e-mails: guy.lagae@ugent.be, wesley.vanlaere@ugent.be, rudy.vanimpe@ugent.be

Keywords: Thin Steel Shells, Stability, Elastic-Plastic Buckling, Plastic Collapse.

Comment. Like Prof. René Maquoi the three authors are active in the field of structural analysis and the design of steel structures. Guy Lagae met Prof. Maquoi during more than twenty years in different technical committees such as TC8 Structural Stability of the ECCS. He knows Prof. Maquoi as a valuable professor and scientist, a hard worker, a kind and always willing person.

Abstract. Frequently the governing failure mode of liquid-filled conical tanks is associated with buckling near the lower rim due to compression of the shell wall in meridional direction notwithstanding the stabilizing tension in circumferential direction. But important axisymmetric imperfections may increase the circumferential tensile stresses in such a way that local yielding precipitates a buckling failure. This failure mode is of the same kind as the “elephant’s foot” buckling at the support of axially compressed thin steel cylinders with internal pressure. This paper gives numerical results for a series of imperfect conical tanks. The collapse is in some cases of the type “elephant’s foot” buckling. The paper explains why the imperfections can cause large circumferential tensile stresses leading to plastic collapse of the tank.

1 INTRODUCTION

A conical shell with a vertical axis of revolution and constant wall thickness is simply supported at the lower end of the cone (Fig. 1). The thin-walled conical shell forms a vessel which contains liquid with a specific weight γ' up to a height h' above the base circle of the cone. The meridional compressive membrane stress increases very rapidly along the generatrices of the cone between the surface of the liquid and the base of the shell. The meridional membrane stress along the bottom edge of the shell of Figure 1 is given by

$$\sigma_x = \frac{\gamma' h'^2 (r_1 + \frac{h'}{3} \tan \beta) \tan \beta}{2 r_1 t \cos \beta} \quad (1)$$

if the weight of the shell is assumed to be negligible compared to that of the liquid. When the level of the liquid in the conical vessel rises gradually, the compressive stresses eventually cause the bottom part of the shell to buckle, in spite of the stabilizing effect of the circumferential tensile stresses σ_θ . Since the load is a gravity load, the shell fails suddenly and catastrophically. The stresses σ are taken positive in the case of compression.

For these liquid-filled conical shells, design rules are available in the Fourth Edition of the ECCS Recommendations of Buckling of Shells [1] and the forthcoming Fifth Edition [2]. The origin of the design rules are the numerous experiments that were performed on scale models. In this paper, the results

of numerical simulations are compared to the stress design procedure of the ECCS and the discrepancy between these two is explained.

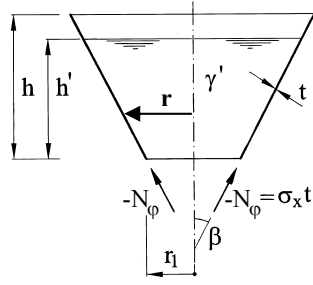


Fig. 1 The cone geometry.

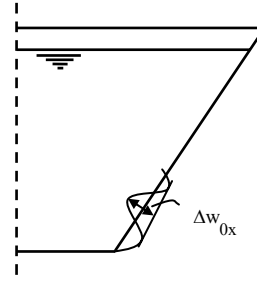


Fig. 2 Measuring the size of the geometric imperfection.

2 STRESS DESIGN

With the design rules given in the forthcoming Fifth Edition of the ECCS Recommendations, a stress design of a liquid-filled conical shell can be performed. The design buckling stress is obtained from

$$\sigma_{xRd} = \frac{\sigma_{xRk}}{\gamma_M} \text{ with } \gamma_M = 1,1. \quad (2)$$

The characteristic buckling stress σ_{xRk} is determined as:

$$\sigma_{xRk} = \chi_{xp} \sigma_{xRpl} \text{ with } \sigma_{xRpl} = \frac{f_{yk}}{\sqrt{1 + \frac{1}{\psi} + \left(\frac{1}{\psi}\right)^2}} \quad (3)$$

with $\psi = \frac{\sigma_x}{|\sigma_\theta|}$, $\sigma_\theta = -\frac{\gamma' h' r_1}{t \cos \beta}$ and f_{yk} the characteristic yield stress.

The relative slenderness ratio is defined as

$$\bar{\lambda} = \sqrt{\frac{f_{yk}}{\sigma_{xRcr}}}. \quad (4)$$

The critical buckling stress of a cone with an angle β and a small radius r_1 under axial compression is given by

$$\sigma_{xRcr} = 0,605 Et \frac{\cos \beta}{r_1}. \quad (5)$$

Eq. (5) provides a good approximation of the meridional buckling stress σ_{xRcr} of a perfect elastic simply supported weightless liquid-filled conical shell.

Reduction factor χ_{xp} :

$$\chi_{xp} = 1 \text{ when } \bar{\lambda} \leq \bar{\lambda}_0 \text{ with } \bar{\lambda}_0 = 0,2 \quad (6)$$

$$\chi_{xp} = 1 - \beta' \left(\frac{\bar{\lambda} - \bar{\lambda}_0}{\bar{\lambda} - \bar{\lambda}_p} \right)^\eta \text{ when } \bar{\lambda}_0 \leq \bar{\lambda} \leq \bar{\lambda}_p \text{ with } \beta' = 1 - 0,5\sqrt{1 + \psi + \psi^2} / \psi \text{ and } \eta = 1,0 \quad (7)$$

$$\chi_{xp} = \frac{\alpha_{xpe}}{\bar{\lambda}^2} \text{ when } \bar{\lambda} \geq \bar{\lambda}_p. \quad (8)$$

The elastic imperfection reduction factor is given by

$$\alpha_{xpe} = 0,50 \cdot \left(1 - \frac{1,50}{Q} \right) \cdot \left(\frac{\gamma' r_1^3}{0,605 \cdot Et^2 \cos^2 \beta} \right)^{0,135(1 + \frac{1,00}{Q})} \text{ or}$$

$$\alpha_{xpe} = 0,50 \cdot \left(1 - \frac{1,50}{Q} \right) \cdot \left(\frac{\omega^2}{605000 \cdot \sqrt{1 - \nu^2}} \right)^{0,135(1 + \frac{1,00}{Q})} \text{ with } \omega = \frac{1000 r_1}{t \cos \beta} \cdot \left[\frac{\gamma' r_1}{E} \sqrt{1 - \nu^2} \right]^{1/2}. \quad (9)$$

$\nu = 0,3$ is the coefficient of Poisson and E is the Young's modulus. The quality parameter Q should be taken from Table 1 for the specified fabrication tolerance quality.

Table 1: Values of fabrication quality parameter Q

| Quality | Description | Q |
|---------|-------------|----|
| Class A | Excellent | 40 |
| Class B | High | 25 |
| Class C | Normal | 16 |

The quality classes are defined in paragraph 8.4 of [3], EN 1993-1-6 Strength and Stability of Shell Structures. In the case where the behaviour is entirely elastic the characteristic buckling stress may alternatively be determined directly from $\sigma_{xRk} = \alpha_{xpe} \cdot \sigma_{xRcr}$.

The value of the plastic limit relative slenderness $\bar{\lambda}_p$ should be determined from:

$$\bar{\lambda}_p = \sqrt{\frac{\alpha}{1 - \beta'}}. \quad (10)$$

It should be verified that $\sigma_{xEd} \leq \sigma_{xRd}$ where σ_{xEd} is the meridional membrane stress at the support due to the liquid filling taken with its design (factored) value.

3 DESIGN BY GLOBAL NUMERICAL ANALYSIS USING GMNIA ANALYSIS

EN 1993-1-6 permits a fully nonlinear analysis, including explicit modelling of geometric imperfections, termed GMNIA (Geometrically and Materially Nonlinear Imperfection Analysis taking into account equivalent imperfections). The first eigenmode found with a LBA (Linear Buckling Analysis) analysis of the perfect shell is used as pattern of the equivalent geometric imperfections. The amplitude of the adopted equivalent geometric imperfections depends on the fabrication tolerance quality class. The maximum deviation of the geometry of the equivalent imperfection from the perfect shape was taken the larger of $\Delta w_{0,eq,1}$ or $\Delta w_{0,eq,2}$, where:

$$\Delta w_{0,eq,1} = \ell_g U_{n1}; \quad (11)$$

$$\Delta w_{0,eq,2} = 25 t U_{n2} . \quad (12)$$

$\ell_g = 4 \sqrt{\frac{r_1 t}{\cos \beta}}$ is the gauge length conformable to paragraph 8.4.4 of EN 1993-1-6. U_{n1} and U_{n2} are the

dimple imperfection amplitude parameters for the relevant tolerance quality class as given in Table 2.

The criteria for collapse in the case of conical tanks are a limit load or a bifurcation. The criterion that limits the most highly stressed point of the shell to first yield is too conservative. The characteristic buckling stress σ_{xRk} is the meridional stress at the base circle corresponding with the liquid level h_{Rk} at collapse.

Table 2: Values for dimple imperfection amplitude parameters

| Fabrication tolerance quality class | Description | Value of U_{n1} | Value of U_{n2} |
|-------------------------------------|-------------|-------------------|-------------------|
| Class A | Excellent | 0,010 | 0,010 |
| Class B | High | 0,016 | 0,016 |
| Class C | Normal | 0,025 | 0,025 |

4 COMPARISON OF STRESS DESIGN AND GMNIA ANALYSIS

4.1 Purpose of the GMNIA calculations

The procedure for liquid-filled conical shells, developed by Prof. D. Vandepitte and described in the Fourth Edition of the ECCS *Buckling of Steel Shells, European Recommendations*, is based on hundreds of experiments performed at the Laboratory for Research on Structural Models of the Ghent University. This procedure was validated in the past by means of numerical simulations with the programs BOSOR (D. Bushnell) [4] and F04B08 (M. Esslinger) [5]. The stress design, explained in section 3, is the transcription of the original procedure of the Fourth Edition of the ECCS Recommendations to the format of EN 1993-1-6 with a slight adaptation allowing the application of the quality classes A, B and C of the EN 1993-1-6. The quality classes A and C correspond to the former classification “good” and “poor” and the quality class B is added by interpolation.

A verification of the stress design procedure has recently been performed with the finite element package ABAQUS [6]. This research is interesting since previous simulations have shown discrepancies between the results with ABAQUS and F04B08 [7].

4.2 Stress design

The water level h'_{rd} corresponding with σ_{xrd} was determined with the stress design procedure for seven cone geometries and for the quality classes A and C (see Table 3).

4.3 Design by global numerical analysis

With the finite element package ABAQUS, the seven geometries were also modelled and the GMNIA analyses for the three quality classes were performed. The critical level of the liquid is obtained by successive approximations. In the first step of the iteration process the height of the liquid h' was h'_{Rcr} corresponding with σ_{xRcr} . These values of h'_{Rcr} are given in Table 3.

For the nonlinear material properties, a perfect elastic-plastic material was assumed: a linear elastic behaviour followed by a plastic horizontal plateau. As explained in section 3 the geometric imperfections were given the shape of the first eigenmode of the perfect cone, which is an axisymmetric mode.

Table 3: Determination of the critical water level for seven cone geometries and for the EC3 quality classes A and C with the stress design procedure

| Number | 1 | 2 | 3 | 4 | 5 | 6 | 7 |
|--|--------------------------------------|---------|---------|---------|---------|---------|---------|
| r_l (mm) | 90 | 3.000 | 350 | 579 | 200 | 3.794 | 3.794 |
| t (mm) | 0,3239 | 10 | 0,30 | 0,310 | 0,1229 | 8 | 15 |
| β (°) | 49,93 | 45 | 40 | 40 | 39,98 | 51 | 51 |
| E (N/mm ²) | 195.420 | 210.000 | 210.000 | 200.000 | 5220 | 196.200 | 196.200 |
| ν | 0,3 | 0,3 | 0,3 | 0,3 | 0,3 | 0,3 | 0,3 |
| f_{yk} (N/mm ²) | 240 | 240 | 240 | 240 | elastic | 240 | 240 |
| ECCS stress design procedure for the liquid-filled conical shell | | | | | | | |
| ω | 28,33 | 155,12 | 190,2 | 401,4 | 1272 | 320,57 | 170,97 |
| Perfect | σ_{xRcr} (N/mm ²) | 274 | 299 | 83,42 | 49,63 | 1,487 | 295,34 |
| | h'_{Rcr} (mm) | 1.234 | 13.222 | 1.464 | 1.322 | 166 | 8.300 |
| Class A | σ_{xRd} (N/mm ²) | 48,45 | 84,69 | 24,96 | 18,24 | 0,7516 | 85,79 |
| | h'_{Rd} (mm) | 664 | 8.032 | 900 | 862 | 121 | 5.350 |
| Class C | σ_{xRd} (N/mm ²) | 43,96 | 78,30 | 23,13 | 17,05 | 0,7112 | 79,41 |
| | h'_{Rd} (mm) | 641 | 7.780 | 872 | 836 | 118 | 5.193 |

The amplitude of the geometric imperfection in the adopted pattern of the equivalent geometric imperfection was interpreted in a manner consistent with the gauge length method, defined in 8.4.4 of EN 1993-1-6 (see Fig. 2). For each geometry, both GMNIA analyses with the first half wave oriented outward and with the first half wave oriented inward were investigated. The lowest collapse load always corresponded with the first half wave oriented outward.

For the GMNIA analyses, the modified Riks algorithm was used. In the analyses, the liquid level was constant and the density of the liquid was increased until bifurcation or a limit load occurred. Eq. (1) was used to determine the meridional compressive stress at the lower rim for the ultimate specific weight γ' and the constant liquid level h' . With this meridional stress, an estimation of the critical water level could be obtained if the specific weight of water was inserted in Eq. (1). For this new liquid level, a new GMNIA analysis was performed and a new ultimate liquid density was obtained. This procedure was repeated until the ultimate density was (almost) equal to the density of water. The results of this iterative process are given in Table 4 for the seven cone geometries and the three quality classes. Also the results of the GMNA analyses for the perfect cones are given, and the results of the GNIA (pure elastic) analyses of the cones of Class C. The parameter λ indicates the ratio of the ultimate density and the water density.

The results in Table 4 for the quality classes A and C can be compared with the results obtained with the stress design procedure taken from the ECCS Recommendations (Table 3). For that purpose, the ratios of σ_{xRd} obtained with numerical simulations and σ_{xRd} obtained with the ECCS procedure are given in Table 5. As can be seen, these ratios are not always equal to or larger than 1. For Class A, the lowest ratio is 0,94, which is still close to unity. For Class C however, the ratio is $\approx 0,60$ for geometry 2, 6 and 7. The ABAQUS analyses show that for these geometries the von Mises stresses at the first axisymmetric bulge close by the lower rim are equal to the yield stress and that this is due to the large circumferential stresses. It is clear that the failure pattern for these cones is “Elephant’s foot” and thus a plastic failure phenomenon.

These results suggest that the ECCS procedure may in some cases overestimate the buckling stress, which is dangerous. However the ECCS procedure is based on a very extensive experimental research, combined with a theoretical investigation, and has thus a solid underpinning. Furthermore, the relevance of the first – axisymmetric – eigenmode as imperfection shape can be argued. It is very unlikely to have an axisymmetric imperfection in practice. And it is precisely the presence of the axisymmetric

imperfection in the numerical simulations that causes the drastic reduction of the buckling stress compared to the one of the perfect cone. This explains why the GMNIA calculations give lower buckling loads than the lower bounds derived from hundreds of tests.

In Table 6, the ratios of the meridional design buckling stresses at the lower rim and the yield stress are given. Although some failure patterns indicate plastic failure, the ratios are smaller than 40% for imperfections of Class A and smaller than 25% for imperfections of Class C. Clearly, due to the presence of the imperfections and the deformations, the actual circumferential stresses are much higher than the theoretical ones and the combination of these actual circumferential and meridional stresses can lead to early yielding and causes the critical water level to be significantly lower than the value predicted with the ECCS procedure for some geometries.

Table 4: Determination of the critical water level for seven cone geometries and for the three EC3 quality classes with ABAQUS

| Number | | 1 | 2 | 3 | 4 | 5 | 6 | 7 |
|-------------------------------|-------------------------------------|---------|---------|---------|---------|---------|---------|---------|
| r_1 (mm) | | 90 | 3.000 | 350 | 579 | 200 | 3.794 | 3.794 |
| t (mm) | | 0,3239 | 10 | 0,30 | 0,310 | 0,1229 | 8 | 15 |
| β (°) | | 49,93 | 45 | 40 | 40 | 39,98 | 51 | 51 |
| E (N/mm ²) | | 195.420 | 210.000 | 210.000 | 200.000 | 5.220 | 196.200 | 196.200 |
| ν | | 0,3 | 0,3 | 0,3 | 0,3 | 0,3 | 0,3 | 0,3 |
| f_{yk} (N/mm ²) | | 240 | 240 | 240 | 240 | elastic | 240 | 240 |
| ABAQUS GMNA | | | | | | | | |
| Perfect | σ_{xRd} (N/mm ²) | 187,24 | 165,66 | 76,00 | 46,56 | 1,42 | 113,82 | 165,15 |
| | h'_{Rd} (mm) | 1.079 | 10.499 | 1.412 | 1.287 | 163 | 7.272 | 10.868 |
| | λ | 1,00 | 1,00 | 0,99 | 1,00 | 1,00 | 1,00 | 1,00 |
| ABAQUS GMNIA | | | | | | | | |
| Class A | σ_{xRd} (N/mm ²) | 90,30 | 81,21 | 31,72 | 23,86 | 1,05 | 53,54 | 80,40 |
| | h'_{Rd} (mm) | 832 | 7.897 | 993 | 968 | 142 | 5.313 | 8.154 |
| | λ | 0,99 | 1,00 | 1,00 | 1,04 | 1,00 | 0,99 | 0,99 |
| Class B | σ_{xRd} (N/mm ²) | 74,10 | 65,05 | 27,06 | 20,49 | 0,94 | 42,42 | 63,88 |
| | h'_{Rd} (mm) | 775 | 7.215 | 931 | 907 | 135 | 4.813 | 7.425 |
| | λ | 1,01 | 1,00 | 1,02 | 0,98 | 0,99 | 0,99 | 0,98 |
| Class C | σ_{xRd} (N/mm ²) | 58,62 | 49,27 | 23,91 | 16,98 | 0,81 | 31,98 | 48,61 |
| | h'_{Rd} (mm) | 712 | 6.436 | 885 | 835 | 126 | 4.263 | 6.637 |
| | λ | 1,01 | 1,00 | 1,03 | 1,01 | 1,02 | 0,99 | 0,99 |
| ABAQUS GNIA | | | | | | | | |
| Class C | σ_{xRd} (N/mm ²) | 63,13 | 111,44 | 23,66 | 18,31 | 0,81 | 67,08 | 112,80 |
| | h'_{Rd} (mm) | 732 | 8970 | 881 | 864 | 125 | 5842 | 9343 |
| | λ | 0,97 | 0,93 | 1,00 | 0,95 | 1,01 | 0,96 | 0,95 |

Table 5: Ratios of design buckling stresses with GMNIA calculations and ECCS procedure

| Number | | 1 | 2 | 3 | 4 | 5 | 6 | 7 |
|--|---------|------|------|------|------|------|------|------|
| $\frac{\sigma_{xRd_GMNIA}}{\sigma_{xRd_ECCS}}$ | Class A | 1,86 | 0,96 | 1,27 | 1,31 | 1,40 | 0,98 | 0,94 |
| | Class C | 1,33 | 0,63 | 1,03 | 1,00 | 1,14 | 0,63 | 0,61 |

Table 6: Ratios of the design buckling stress at the lower rim and the yield stress

| Number | | 1 | 2 | 3 | 4 | 5 | 6 | 7 |
|--------------------------------------|---------|------|------|------|------|---|------|------|
| $\frac{\sigma_{xRd_GMNIA}}{f_{yk}}$ | Class A | 0,38 | 0,34 | 0,13 | 0,10 | - | 0,22 | 0,33 |
| | Class C | 0,24 | 0,21 | 0,10 | 0,07 | - | 0,13 | 0,20 |

Table 7 shows that in the case of pure elastic behaviour the ECCS procedure leads to safe results for *all* the geometries even for the quality class C.

Table 7: Ratios of design values of the stresses with GNIA calculations and ECCS procedure

| Number | | 1 | 2 | 3 | 4 | 5 | 6 | 7 |
|---------|---|------|------|------|------|------|------|------|
| Class C | $\sigma_{xRd_GNIA} / \sigma_{xRd_ECCS}$ | 1,44 | 1,42 | 1,02 | 1,07 | 1,14 | 1,32 | 1,42 |

5 ORIGIN OF THE LARGE CIRCUMFERENTIAL STRESSES IN IMPERFECT CONICAL TANKS

With the characteristic buckling stress $\sigma_{xRk} = \gamma_m \cdot \sigma_{xRd} = 1,1 \cdot 49,27 = 54,20 N/mm^2$ for cone 2 and quality class C in Table 4 corresponds a characteristic water level $h'_{Rk} = 6705 mm$. With this water level corresponds a circumferential stress

$$\sigma_{\theta} = -\frac{\gamma' h' r_1}{t \cos \beta} = -\frac{9,81 \cdot 10^{-6} \cdot 6705 \cdot 3000}{10 \cdot \cos 45^\circ} = -27,90 N/mm^2$$

if the membrane theory is applied, the geometrical imperfections of the conical tank are neglected and the principal radii of curvature $R_1 = \infty$ and $R_2 = r_1 / \cos \beta$ are used in the well known formula for shells of revolution loaded symmetrically with respect to their axis

$$\frac{N_{\varphi}}{R_1} + \frac{N_{\theta}}{R_2} = Z. \quad (13)$$

$N_{\varphi} = -\sigma_x \cdot t$ and $N_{\theta} = -\sigma_{\theta} \cdot t$ denote the magnitudes of the membrane forces, per unit length, in the meridional and the circumferential direction. $Z = \gamma' h'$ is the component of the external load normal to the surface of the shell. The corresponding von Mises stress is

$$\sigma_{eq} = \sqrt{\sigma_x^2 + \sigma_{\theta}^2 - \sigma_x \cdot \sigma_{\theta}} = 72,30 N/mm^2 \quad (14)$$

and doesn't attain the yield stress as in the GMNIA calculation.

The formula (13) is now applied taking into account the axisymmetric initial geometrical imperfections of quality class C plus the deformations of the shell wall at the start of yielding in the mid surface of the shell. The GMNIA calculation shows that yielding of the mid surface starts for a load factor 0,967 and that the corresponding deformations in the vicinity of the base circle of the conical tank can be approximated by the initial geometrical imperfections multiplied by 0,35. The deviation of the deformed meridian of the conical tank from the straight line is approximated by :

$$y = (1 + 0,35) \cdot \frac{0,025 \cdot l_g}{2} \cdot \sin \frac{2\pi x}{l_g} \quad (15)$$

where $0,025 \ell_g$ represents the amplitude of the assumed initial sinusoidal imperfection and $\ell_g = 4 \sqrt{\frac{r_1 t}{\cos \beta}} = 824 \text{ mm}$ the gauge length. The first half wave is taken in outward direction. The coordinate x is measured along the meridian. The maximum curvature of the meridian is $y''_{\max} = -\frac{1,35 \cdot 0,025 \cdot 2 \cdot \pi^2}{\ell_g} = -\frac{0,6662}{824}$ and the corresponding principal radius of curvature of the shell wall $R_1 = \frac{1}{|y''_{\max}|} = \frac{824}{0,6662} = 1237 \text{ mm}$. At that location x is $824/4 = 206 \text{ mm}$, the radius of the parallel circle $r = 3000 + 206 \cdot \sin 45 = 3146 \text{ mm}$, the principal radius $R_2 \cong r / \cos 45^\circ = 4449 \text{ mm}$ and the water height $h' = 6705 - 206 \cdot \cos 45^\circ = 6559 \text{ mm}$. We calculate meridional membrane stress σ_x at that location by writing the equilibrium of the shell above the parallel circle

$$\sigma_x = \frac{\gamma' h'^2 (r + \frac{h'}{3} \tan \beta) \tan \beta}{2 r t \cos \beta} = \frac{9,81 \cdot 10^{-6} \cdot 0,967 \cdot 6559^2 \cdot (3146 + \frac{6559}{3} \tan 45^\circ) \cdot \tan 45^\circ}{2 \cdot 3146 \cdot 10 \cdot \cos 45^\circ} = 48,91 \text{ N/mm}^2$$

The application of formula (13) in the deformed state of the shell gives

$$\frac{N_\varphi}{R_1} + \frac{N_\theta}{R_2} = Z = \frac{-\sigma_x \cdot 10}{1237} + \frac{-\sigma_\theta \cdot 10}{4449} = 9,81 \cdot 10^{-6} \cdot 0,967 \cdot 6559$$

$$\sigma_\theta = -444,9 \cdot (0,0622 + 0,3954) = -203,6 \text{ N/mm}^2$$

The corresponding von Mises stress is given by

$$\sigma_{eq} = \sqrt{\sigma_x^2 + \sigma_\theta^2 - \sigma_x \cdot \sigma_\theta} = \sqrt{48,91^2 + (-203,6)^2 - 48,91 \cdot (-203,6)} = 232,1 \text{ N/mm}^2$$

and matches very well the equivalent stress f_{yk} obtained in the GMNIA calculation. Although this result confirms our statement that the early yielding is caused by the enlarged circumferential stresses due to the imperfections and deformations, the accuracy of the analytical method that is used here is limited. The shape of the first eigenmode and the deformations are approximated by a sine wave. A membrane analysis is used and the disturbance of the membrane state by the adjacent boundary conditions is neglected... The main lesson of this analytical method is that the presence of the imperfection leads to very large circumferential stresses which – in combination with the meridional stresses – can lead to early yielding.

The method can also be used when the first half wave is taken inwards. In this case the sign of the R_1 changes and the new values for the stresses are

$$\sigma_\theta = -444,9 \cdot (0,0622 - 0,3954) = 148,2 \text{ N/mm}^2 \text{ (compression) and}$$

$$\sigma_{eq} = \sqrt{48,91^2 + (148,2)^2 - 48,91 \cdot (148,2)} = 130,8 \text{ N/mm}^2$$

This confirms that in the case of “elephant’s foot” buckling initial geometric imperfections with the first half wave outwards are more detrimental than imperfections with the first half wave inwards.

With this approximate calculation the unexpected large circumferential stresses in conical tanks with large axisymmetric imperfections are explained. This approximate calculation doesn’t claim any accuracy but allows to understand the origin of large circumferential stresses and can be used to evaluate the risk for “elephant’s foot” buckling.

6 INVESTIGATION OF OTHER IMPERFECTION SHAPES

6.1 Realistic imperfection shapes

In [3] guidelines are given for the choice of equivalent geometric imperfections in GMNIA analyses. Basically, since in many cases this is the most unfavourable pattern, an eigenmode-affine pattern is recommended, unless such a pattern can be eliminated for being unrealistic. Based on these recommendations, the authors already mentioned in section 4 that the first eigenmode of the cone – which is an axisymmetric one – is probably not a realistic pattern and that the results of the GMNIA analyses should be put in perspective.

In order to validate the design procedure of the ECCS Recommendations [2], two other imperfection shapes and the results of the corresponding GMNIA analyses are studied here. For that purpose, the geometry of cone 2 and quality class C is chosen. These somewhat more realistic imperfection shapes are shown in Fig. 3. In Fig. 3(b) the 15th eigenmode of cone 2 is given. This eigenmode is chosen for the rather large number of waves in circumferential direction in combination with the waves in meridional direction. In Fig. 3(c), the second imperfection shape is presented. This shape represents a local dimple in the cone wall near the lower rim.

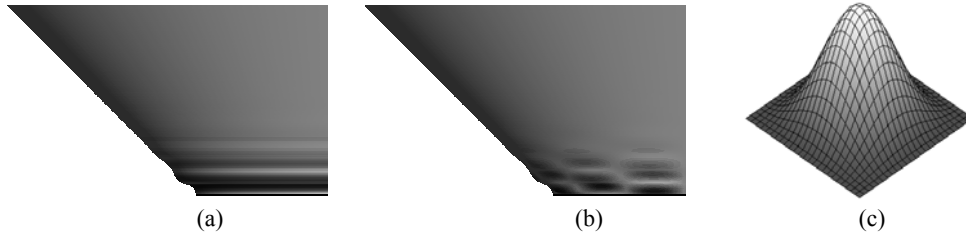


Fig. 3 The three imperfection studied. (a) The first eigenmode – axisymmetric, (b) the 15th eigenmode with waves in circumferential and meridional direction, (c) the local dimple.

6.2 Eigenmode with waves in circumferential and meridional direction as imperfection shape

The new GMNIA analysis was performed on an imperfect cone with the dimensions of geometry 2 as given in Table 4. In this table, the results of the GMNIA analyses with the axisymmetric imperfection (Fig. 3(a)) are presented. These results lead to a characteristic water level of 6705 mm in combination with an ultimate liquid density equal to the density of water. In order to reduce the number of simulations, the iterative procedure of section 4.3 is abandoned and replaced by GMNIA analyses with constant liquid level. The parameter that is varied is the liquid density. The stress design for this liquid level, geometry 2 and quality Class C leads to a characteristic ultimate liquid density that is 1,71 times larger than the density of water.

In order to check whether a more realistic imperfection shape leads to an ultimate liquid density that is larger than the value given by the ECCS procedure, a new eigenmode was chosen rather randomly. The 15th eigenmode is shown in Fig. 3(b) and is characterised by buckles in circumferential and meridional direction. The amplitude of the imperfection is the maximum equivalent amplitude corresponding to Class C. With these characteristics, the GMNIA analysis led to an ultimate liquid density that is equal to 1,72 times the liquid density. This means that the ECCS procedure leads to a slightly conservative value.

6.3 Local dimple as imperfection shape

The second alternative imperfection shape that was investigated is a local dimple with a sinusoidal shape with wavelength ℓ_g in both circumferential and meridional direction (Fig. 3(c)). The dimple was placed just above the lower rim and the amplitude was equal to the maximum equivalent amplitude corresponding to Class C. The GMNIA analysis for this imperfection shape gave an ultimate liquid

density of 2,54 times the water density if the imperfection was oriented outward and an ultimate liquid density of 2,63 times the water density if the imperfections was oriented inward.

6.4 Discussion of imperfection study

In Fig. 3, the three imperfection shapes studied are shown. It is clear that based on this rather limited study no definitive conclusions can be drawn. Nevertheless, some tendencies can be seen. With an axisymmetric imperfection the consequences for the structural behaviour are dramatic. The circumferential stresses are severely increased and the danger of yielding is obvious. This behaviour is not covered by the ECCS Recommendations. However, an axisymmetric buckling shape as imperfection is not realistic. With the non axisymmetric imperfections studied so far, the results show that the ECCS procedure leads to a lower bound. However, other shapes should be studied before solid conclusions can be made.

7 CONCLUSION

The numerical simulations of conical tanks with large axisymmetric imperfections lead in some cases to unexpected low buckling stresses due to local yielding of the type “elephant’s foot” buckling. An approximate analytical method shows that these important axisymmetric imperfections increase the circumferential stresses in such a way that local yielding precipitates the buckling failure.

8 ACKNOWLEDGEMENTS

The transcription of the ECCS rules of the fourth edition into the format of the forthcoming fifth edition was realised in intensive cooperation with Prof. Werner Guggenberger of TU Graz. Most of the numerical calculations, needed for this paper, were performed by ir. Tom De Clippeleir in the framework of his Master Thesis [8]. The authors gratefully acknowledge their support. The second author is a Postdoctoral Fellow of the Research Foundation – Flanders (FWO). Therefore, the authors would like to express their gratitude for the financial support of the FWO.

REFERENCES

- [1] Technical working group on the stability of shells, Buckling of Steel Shells, European Recommendations, Fourth edition, No 56, European Convention for Constructional Steelwork, Brussels, 1988.
- [2] Technical working group on the stability of shells of the ECCS, Sixth and provisional draft of the 5th edition of “Buckling of Steel Shells, European Recommendations”, April 2007.
- [3] EN 1993-1-6, 2006, *Eurocode 3: Design of steel structures-part 1-6: Strength and Stability of Shell Structures*, CEN, European Committee for Standardization, Central Secretariat: rue de Stassart 36, B-1050 Brussels.
- [4] Bushnell D., *Computerized buckling analysis of shells*, Martinus Nijhoff Publishers, Dordrecht, Boston, Lancaster, 1985.
- [5] Esslinger M., Geier B., Wendt U., “Berechnung der Spannungen und Deformationen von Rotationsschalen im elasto-plastischen Bereich”, *Stahlbau*, 1/1984, 17-25.
- [6] ABAQUS, Hibbitt, Karlsson & Sorenson, Inc. E-mail: info@abaqus.com, support@abaqus.com, <http://www.abaqus.com>.
- [7] Lagae G., Van Impe R., Buffel P., Vanlaere W., “Comparison of design buckling stresses for liquid-filled cones obtained with two different procedures”, *Proceedings of the Third European Conference on steel structures*, Coimbra (19-20/9), Portugal, 493-502, 2002.
- [8] De Clippeleir T., “Invloed van geometrische imperfecties bij hydrostatische belaste kegelschalen”, Master Thesis, Faculty of Engineering, Ghent University, June 2007.